Journal of Mines, Metals and Fuels, *71(11): 2319-2326; 2023. DOI: 10.18311/jmmf/2023/36257*

Print ISSN : 0022-2755

Journal of Mines, Metals and Fuels

Contents available at: *www.informaticsjournals.com/index.php/jmmf*

Synthesis and Characterization of Reduced Graphene Oxide Fabricated Over Ruthenium Oxide through Reflux Method

S. Chandruvasan[1], M. Mylarappa[1]*, S. G. Prasanna Kumar[2], S. Kantharaju[1] and K. N. Shravana Kumara[3]

[1]Department of Chemistry, SJR of Science, Arts and Commerce, Bengaluru - 560009, Karnataka, India; mylu4mkallihatti@gmail.com

[2]Department of Chemistry, MS Ramaiah College of Arts, Science and Commerce, Bengaluru - 560054, Karnataka, India

[3]Maharani Lakshmi Ammanni College for Women (Autonomous), Bengaluru - 560012, Karnataka, India

Abstract

In this present work, graphene supported ruthenium oxide (rGO/RuO_2) was synthesized by reflux method. Spectroscopic techniques were used to characterize the synthesized rGO/RuO_2 NPs, including Fourier Transform Infrared (FT-IR), Scanning Electron Microscopy (SEM), X-Ray Diffraction (XRD), and Energy-Dispersive X-ray (EDAX). Synthesized rGO/RuO_2 NPs that were prepared via reflux method at 150 °C for 3 hours showed a paper like structure with an average crystalline sizes of reduced graphene and rGO/RuO_2 was found to be 14 and 10.3 nm. Therefore, the reflux synthesis method, as compared to more complex and time-consuming synthesis methods, can be used to easily and quickly produce high-quality, uniform-sized rGO/RuO_2 NPs. The synthesized material has a successful application in electrochemical sensors, photocatalyst, antioxidant, hydrogen generation, used as catalyst in mines, minerals and fuels.

Keywords: *Characterization, rGO, Reflux Method, rGO/RuO_2*

1.0 Introduction

In every aspect of life, materials made of graphene play a significant role. One of these relatively new wonder materials is graphene. It is the thinnest, most transparent, strongest, and most conductive material, and as a result, it has numerous applications in the electronics industry[1]. Graphene and its various derivatives have so many unique and advantageous properties, there has been a lot of research into using them. These substances may be utilized alone or in conjunction with other nanomaterials, such as nanoparticles. Based on their structural morphology, graphene-nanoparticle hybrid materials may be generally classified into two main types. There are two types of them: There are two types of graphene nanoparticles: (1) Nanoparticles are synthesized or manufactured on sheets of graphene or its derivatives to create composite materials of graphene. The primary distinction between these two groups is the size ratio between the diameter of the nanoparticles and the lateral dimensions of the graphene sheets. The nanoparticles are often modest in size compared to the graphene sheets and are readily decorated onto the sheets to create graphene-nanoparticle composites. This is especially true when their diameter

*Author for correspondence

is between a few nanometers and roughly a hundred nanometers. On the other hand, when the nanoparticles are larger and more comparable in size to the graphene sheets, tiny 2D sheets can be wrapped around them to create graphene-encapsulated nanoparticles. The main processes for producing graphene, GO and rGO will be briefly discussed at the outset of this section. The various techniques for creating hybrid structures made of graphene and nanoparticles will then be thoroughly examined, with an emphasis on the properties and traits that each of these processes produces[2]. Ruthenium oxide (RuO_2) is significant in science and technology due to a variety of properties, including low resistivity, chemical and thermal stability and various other properties[3-4]. For instance, hydrous RuO_2 has been used as a well-known super capacitor electrode because of both its excellent specific capacitance and its lengthy cycle life[5]. They also hold a great deal of interest because of the various field in which they have applications, including microelectronics, electrochemical capacitors, and catalysis[6]. In the chlor-alkali industry, dimensionally stable anodes commonly feature RuO_2 as the primary active component. Furthermore, this compound is utilized in various other applications, such as CO oxidation within sensors and the reduction of CO_2 in photocatalysis processes. The development of more effective and dependable processes for producing RuO_2 nanomaterials has recently been the focus of research. Several research studies have been undertaken to analyze the synthesis methods, electrochemical traits, crystalline structure, and surface morphology. The objective is to gain a comprehensive understanding of the chemical mechanisms that underlie the previously mentioned applications. This pursuit is driven by the diverse uses and extensive versatility associated with ruthenium oxides[7-8]. Hydrous ruthenium oxides are produced in this way. Typically, there is no observable X-ray diffraction pattern in hydrous oxide due to its completely amorphous nature[9]. When hydrous oxide is heated to temperatures above 300 °C, the solid phase dehydrates and forms rutile crystals, which have the chemical formula RuO_2[10]. Ruthenium oxide complex is formed in 2 oxide phases specifically Ru(IV) and (III) in RuO_2 according to XPS and CV[11].

It can ensure that the electrolyte is exposed to enough electroactive sites to start the Faradaic redox reaction[12]. Nanostructured electrode materials are made by mixing specific carbon-based substances with nanostructured metal oxides. These substances include carbon nanotubes, activated carbon and carbon nanofibers[13-14]. The precursor to graphene, graphene oxide, has a lot of oxygen-containing functional groups on its surface. Combining ruthenium oxide and graphene can result in a three-dimensional conductive network, a larger specific surface area, and an improvement in the system's conductivity. However, the severe aggregation of RuO_2 nanoparticles (NPs) in these composites frequently leads to low capacitance[15]. Reduced Graphene Oxide (rGO) and Ruthenium Dioxide (RuO_2) exhibit remarkable properties that find applications in the realms of mines, minerals, and fuels. rGO, derived from graphene oxide, offers exceptional conductivity and surface area, proving instrumental in sensing gases like methane and carbon monoxide for enhanced mine safety.

Moreover, its adsorption capabilities aid in wastewater treatment, effectively removing heavy metals and pollutants generated by mining operations, thereby contributing to environmental preservation. On the other hand, RuO_2, known for its catalytic prowess, plays a pivotal role in mining processes such as hydrometallurgy, facilitating metal extraction from ores and purifying minerals. Beyond mining, RuO_2-based electrodes in fuel cells contribute to efficient energy conversion and storage, impacting the fuel industry positively[18].

The integration of rGO and RuO_2 showcases their potential to improve safety, environmental impact, and industrial processes within these sectors, underlining their significance in advancing mining, mineral extraction, and energy-related technologies[15-17]. In the Present study, rGO/RuO_2 was synthesized by using reflux method which is economically and environmentally friend method by using less chemicals. The materials have been characterized through SEM, EDAX, FTIR and XRD, the materials have a potential application in electro photocatalyst, photocatalyst, corrosion, antioxidant and various other studies and application.

2.0 Chemicals and Methods

2.1 Synthesis of GO

2 g of graphite powder and 1g of $NaNO_3$ were mixed in a 500 mL beaker that was immersed in an ice bath and kept

Table 1. Chemicals used in the experiment.

Materials	Formula	Specification (g/mol)	Suppliers
Sodium Nitrate	$NaNO_3$	84.9	Merck, Bengaluru
Sulphuric acid	H_2SO_4	39.9	Merck, Bengaluru
Hydrogen peroxide	H_2O_2	34.01	Merck, Bengaluru
Potassium Permanganate	$KMnO_4$	158.0	Merck, Bengaluru
Ruthenium chloride	$RuCl_3$	207.4	Merck, Bengaluru
Tri-Sodium citrate	$Na_3C_6H_5O_7$	294.1	Merck, Bengaluru
Sodium sulphite	Na_2SO_3	126.0	Merck, Bengaluru
Ammonia	NH_3	17.03	Merck, Bengaluru

between 0 and 6°C. Then 98% H_2SO_4 was gradually added. The reaction mixture and ice bath were continuously stirred with a magnetic stirrer. After 3 hours, add 6 g of $KmnO_4$ to the mixture gradually. Because $KMnO_4$ causes the mixture to spill and effervesce, it is critical to take precautions to avoid an explosion. After two hours, the beaker was taken out of the ice bath and put on a hot plate with a magnetic stirrer to keep the temperature at 30 degrees Celsius. Due to the rise in temperature increased gradually increased every half hour as the colour turned brownish black. After two hours, add 100 mL of water while continuously stirring, then turn off the heat. About, 80 ml of H_2O_2 was added to the reaction solution. A yellow-coloured solution is formed. The sample obtained was filtered and calcined at 100 ^0C[16-17].

2.2 Synthesis of rGO/RuO_2

In a standard synthesis method, 50 ml of water and 0.1 M of $RuCl_3.H_2O$ were thoroughly combined under stirring using a magnetic stirrer for an hour. The reduced Graphene Oxide (rGO) solution was prepared by blending 5 mg of rGO powder with 20 ml of water. The freshly made NH_3 was continuously stirred to facilitate the exfoliation of the rGO powder. Subsequently, the mixture was transferred to a 100 ml round-bottom flask and refluxed for approximately 3 hours. The resulting solution was then filtered, and the filtrate was dried in a hot air oven at 150 °C for 20 minutes[18].

3. Results and Discussion

3.1 XRD

Figure 1 (a) and 1 (b) shows, respectively, the XRD of rGO and rGO/RuO_2. The avgerage particle diameters of the particles were determined using Scherer's equation[19-20]. The rGO and rGO/RuO_2 calculated mean crystallite were to be 14 and 10.3 nm, respectively. The rGO/RuO_2 XRD pattern shows sharper, more intense peaks, which indicates that the prepared sample has good crystallinity.

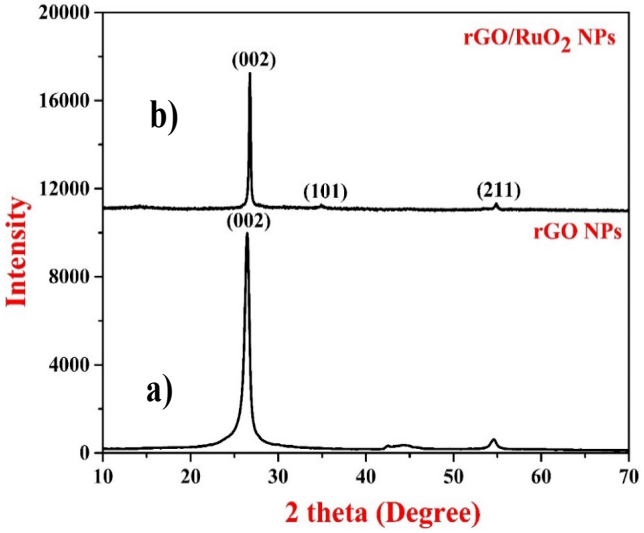

Figure 1. The XRD of rGO and rGO/RuO_2.

There was no sign of impurity peaks, which suggested a high level of purity. The strong and narrow peak of the synthesised product indicates that the particles are well-formed crystals[21].

3.2 SEM

The rGO and rGO/RuO_2 surface morphology was observed using SEM analysis, as in Figure 2 (a) and 2 (b), respectively. SEM of rGO in the Figure 2 (a) that particles are well distributed over the area, the reduced graphene look like a paper or sheet like structure which was overstocked over one another this indicates that it's a single layer of graphene[24]. In Figure 2 (b) shows the SEM image of rGO/RuO_2 clearly that RuO_2 was like an uneven Spherical shape like structures over the reduced graphene as a result due to homogenous layer of reduced graphene oxide the ruthenium oxide particle well dispersed over the surface[22-23].

3.3 EDAX

EDAX images of the prepared sample were used to verify the presence of C, Ru and O. The graphene layers that make up the rGO/RuO_2 composite's morphology were found to be agglomerated with RuO_2 nanoparticles as shown in Figure 3 (b). The sheet-like structure of graphene with RuO_2 attached to its surface is confirmed by a higher magnification image. The aggregation of RuO_2 with graphene due to an increase in graphene weight percent results in an irregular flake-like morphology for the graphene structure, as seen in the magnified image[25].

3.4 FTIR

The FTIR studies shows the presence of strong and weak vibration are observed in the synthesised rGO and rGO/RuO_2 NPs was identified as indicated in Figure 4 (a) to Figure 4 (b). In the Figure 4 (a) rGO NPs the

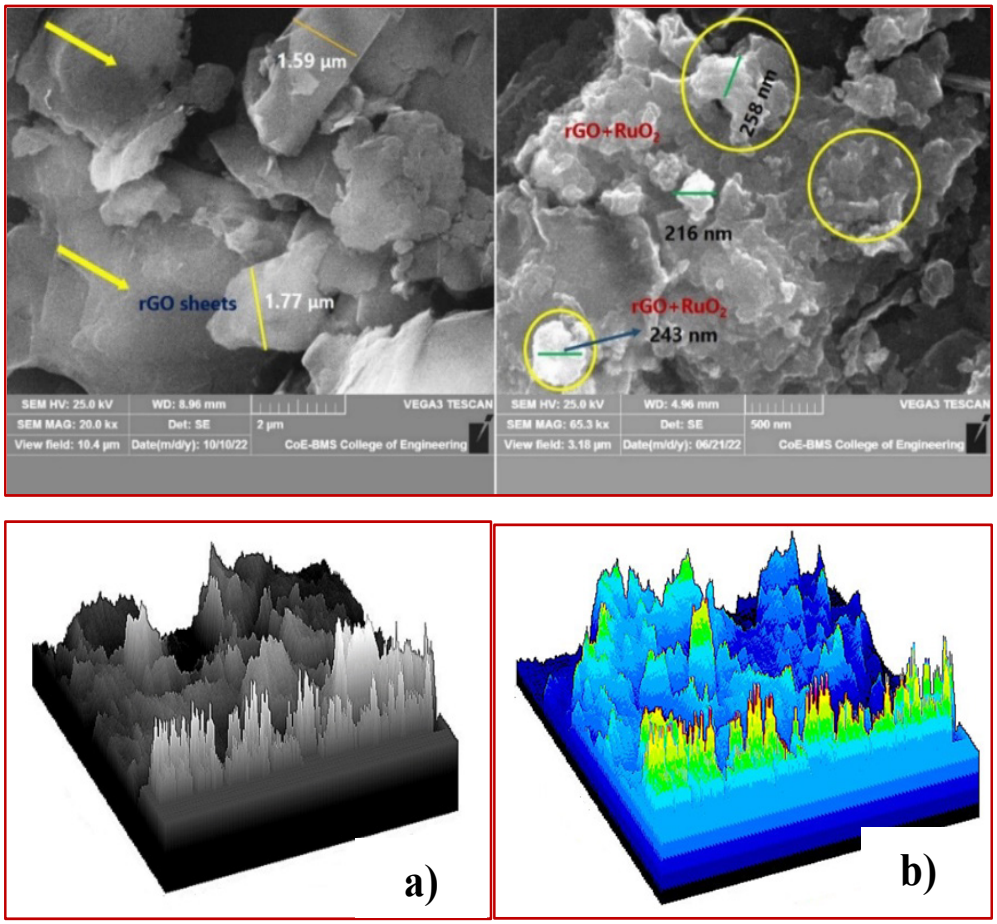

Figure 2. SEM of a) rGO b) rGO/RuO_2.

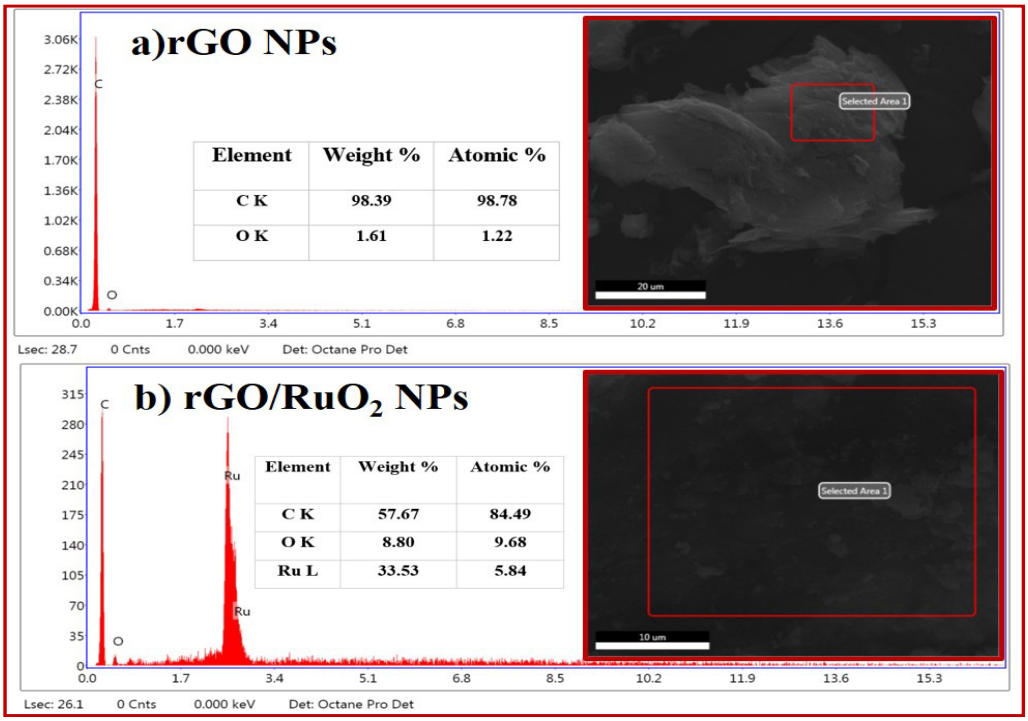

Figure 3. EDAX of a) rGO b) rGO/RuO_2.

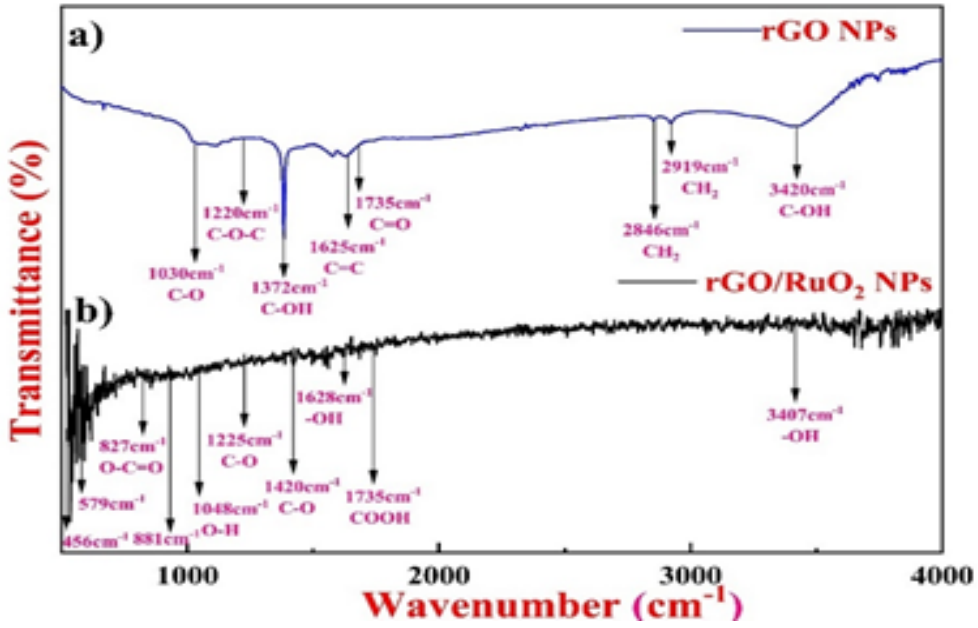

Figure 4. FTIR of (a) rGO (b) rGO/RuO_2

stretching vibrations of the -OH bond in C-OH groups are represented by a broad band at 3420 cm^{-1}, which may be influenced by water and carboxylic acids. Stretching vibrations of CH_2 are responsible for the two minor

peaks at 2918 and 2846 cm^{-1}. The peak at 1735 cm^{-1} is due to the stretching of the carboxylic functionalities (-COOH) with carbonyl/carboxyl groups (C=O), which are most likely present at the sheet edges. Stretching in the C=C bond's sp^2 vibration plane is the cause of the peak at 1625 cm^{-1}. Peaks at 1372 cm^{-1} and 1220 cm^{-1}, respectively, are related to bending vibrations of C-OH hydroxyl groups and epoxy groups (C-O-C), respectively. The C-O vibration of epoxy, ether, or peroxide groups causes the peak at 1030 cm^{-1}. The stretching vibrations of the rGO/RuO_2 NPs are visible in Figure 4 (b). The weak band nearby at 579 cm^{-1} and the small band at 456 cm^{-1} are linked to RuO_2's distinctive asymmetric stretching mode. The Vibration peak at 881 cm^{-1} is for the presence of Ru-OH traces. The two absorption bands at 1067 cm^{-1} and 1735 cm^{-1} are thought to be responsible for the per oxo groups' distinctive stretching vibration. The absorption band at 1628 cm^{-1} is created by the molecular water's hydroxyl groups vibrating. The broad absorption band at 3407 cm^{-1} is caused by the OH group's stretching vibrations. The study shows a strong band of RuO_2 in FTIR studies[26-30].

4.0 Conclusion

The reflux method was used to prepare the rGO/RuO_2. XRD, SEM, FTIR, and EDAX spectra were used to examine the composite morphology and structure. The results of these characterization studies demonstrate that the particles are crystalline and evenly dispersed throughout the composite and they also allow for the detection of functional groups and the derivation of elemental composition studies. As a result, the prepared compound has an excellent usefulness in the electrocatalysts, photocatalyst, antioxidant, minerals preparation applications.

5.0 Acknowledgment

The authors express their gratitude to the SJR college and the Principal of SJR College in Bengaluru for their unwavering encouragement and support throughout the successful completion of the research work.

6.0 References

1. Morozov SV, Novoselov KS, Katsnelson MI, Schedin F, Elias DC, Jaszczak JA, *et al*. Giant intrinsic carrier mobilities in graphene and its bilayer. Phys Rev Lett. 2008; 100:016602. https://doi.org/10.1103/PhysRevLett.100.016602.
2. Yin PT, Shah S, Chhowalla M, Lee K-B. Design, synthesis, and characterization of graphene–nanoparticle hybrid materials for bioapplications. Chem Rev. 2015; 115:2483–531. https://doi.org/10.1021/cr500537t.
3. Bi R-R, Wu X-L, Cao F-F, Jiang L-Y, Guo Y-G, Wan L-J. Highly dispersed ruo$_2$ nanoparticles on carbon nanotubes: facile synthesis and enhanced supercapacitance performance. J Phys Chem C. 2010; 114:2448–51. https://doi.org/10.1021/jp9116563.
4. Subhramannia M, Balan BK, Sathe BR, Mulla IS, Pillai VK. Template-assisted synthesis of ruthenium oxide nanoneedles: electrical and electrochemical properties. J Phys Chem C. 2007; 111:16593–600. https://doi.org/10.1021/jp0744836.
5. Kim J-Y, Kim K-H, Yoon S-B, Kim H-K, Park S-H, Kim K-B. In situ chemical synthesis of ruthenium oxide/reduced graphene oxide nanocomposites for electrochemical capacitor applications. Nanoscale. 2013; 5:6804. https://doi.org/10.1039/c3nr01233f.
6. McKeown DA, Hagans PL, Carette LPL, Russell AE, Swider KE, Rolison DR. Structure of Hydrous Ruthenium Oxides: Implications for Charge Storage. J Phys Chem B. 1999; 103:4825–32. https://doi.org/10.1021/jp990096n.
7. Zheng JP, Cygan PJ, Jow TR. Hydrous Ruthenium Oxide as an Electrode Material for Electrochemical Capacitors. J Electrochem Soc. 1995; 142:2699–703. https://doi.org/10.1149/1.2050077.
8. Hu C-C, Huang Y-H. Effects of preparation variables on the deposition rate and physicochemical properties of hydrous ruthenium oxide for electrochemical capacitors. Electrochimica Acta. 2001; 46:3431–44. https://doi.org/10.1016/S0013-4686(01)00543-6.
9. Málek J, Watanabe A, Mitsuhashi T. Crystallization kinetics of amorphous RuO_2. Thermochimica Acta. 1996; 282–283:131–42. https://doi.org/10.1016/0040-6031(96)02887-0.
10. Kötz R, Lewerenz HJ, Stucki S. XPS Studies of Oxygen Evolution on Ru and RuO_2 Anodes. J Electrochem Soc 1983; 130:825–9. https://doi.org/10.1149/1.2119829.

11. Ghasemi S, Ahmadi F. Effect of surfactant on the electrochemical performance of graphene/iron oxide electrode for supercapacitor. Journal of Power Sources. 2015; 289:129–37. https://doi.org/10.1016/j.jpowsour.2015.04.159.
12. Guo D, Luo Y, Yu X, Li Q, Wang T. High performance $NiMoO_4$ nanowires supported on carbon cloth as advanced electrodes for symmetric supercapacitors. Nano Energy. 2014; 8:174–82. https://doi.org/10.1016/j.nanoen.2014.06.002.
13. Wu HB, Xia BY, Yu L, Yu X-Y, Lou XW. Porous molybdenum carbide nano-octahedrons synthesized via confined carburization in metal-organic frameworks for efficient hydrogen production. Nat Commun. 2015; 6:6512. https://doi.org/10.1038/ncomms7512.
14. Dai C-S, Chien P-Y, Lin J-Y, Chou S-W, Wu W-K, Li P-H, *et al*. Hierarchically structured Ni_3S_2 /Carbon Nanotube Composites as High Performance Cathode Materials for Asymmetric Supercapacitors. ACS Appl Mater Interfaces. 2013; 5:12168–74. https://doi.org/10.1021/am404196s.
15. Ates M, Yildirim M, Kuzgun O, Ozkan H. The synthesis of rGO, rGO/RuO_2 and rGO/RuO_2/PVK nanocomposites, and their supercapacitors. Journal of Alloys and Compounds. 2019; 787:851–64. https://doi.org/10.1016/j.jallcom.2019.02.126.
16. Mylarappa M, Chandruvasan S, Kantharaju S, Rekha S. Synthesis and characterization of Rgo doped Nb_2O_5 nano composite for chemical sensor studies. ECS Trans. 2022; 107:269–75. https://doi.org/10.1149/10701.0269ecst.
17. Mylarappa M, Rekha S, Kantharaju S, Chandruvasan S, Shravana KN. Synthesis and characterization of ZnO and MgO nanoparticles through green approach and their antioxidant properties. ECS Trans. 2022; 107:689–95. https://doi.org/10.1149/10701.0689ecst.
18. Mylarappa M, Chandruvasan S, Thippeswamy B, Shravana Kumara KN, Kantharaju S. Clay incorporated ruthenium oxide nanocomposite for electrochemical, sensor, optical, photocatalytic and antioxidant studies. Sustainable Chemistry for the Environment. 2023; 2:100007. https://doi.org/10.1016/j.scenv.2023.100007.
19. Mylarappa M, Raghavendra N, Surendra BS, Shravana Kumar KN, Kantharjau S. Electrochemical, photocatalytic and sensor studies of clay/MgO nanoparticles. Applied Surface Science Advances. 2022; 10:100268. https://doi.org/10.1016/j.apsadv.2022.100268.
20. Cruz M, Gomez C, Duran-Valle CJ, Pastrana-Martínez LM, Faria JL, Silva AMT, *et al*. Bare TiO_2 and graphene oxide TiO_2 photocatalysts on the degradation of selected pesticides and influence of the water matrix. Applied Surface Science. 2017; 416:1013–21. https://doi.org/10.1016/j.apsusc.2015.09.268.
21. Mylarappa M, Chandruvasan S, Harisha KS, Shravana Kumara KN. Ajwain honey loaded CeO_2 nanocomposite for antioxidant, chemical sensors and photocatalysis studies. Kuwait Journal of Science. 2023:S2307410823001864. https://doi.org/10.1016/j.kjs.2023.10.012.
22. Daolio S, Kristóf J, Piccirillo C, Pagnra C, De Battisti A. Investigation of the formation of RuO_2 -based mixed oxide coatings by secondary ion mass spectrometry. J Mater Chem. 1996; 6:567–71. https://doi.org/10.1039/JM9960600567.
23. Mylarappa M, Chandruvasan S, Harisha KS, Kantharaju S, Prasanna Kumar SG, Shravana Kumara KN. Development of Coriander Honey loaded CeO_2 for cyclic voltammetry, chemical sensor, dye purification, and antioxidant properties. Journal of the Taiwan Institute of Chemical Engineers. 2023; 152:105174. https://doi.org/10.1016/j.jtice.2023.105174.
24. Daolio S, Kristóf J, Piccirillo C, Pagnra C, De Battisti A. Investigation of the formation of RuO_2 -based mixed oxide coatings by secondary ion mass spectrometry. J Mater Chem. 1996; 6:567–71. https://doi.org/10.1039/JM9960600567.
25. Chandruvasan S, Madival H, Mylarappa M, Naik ND, Kantharaju S, Bharath S. Investigation of antioxidant and photo catalysis of natural honey and cow urine-doped CeO_2 nanoparticles fabricated by reflux method. Engineering, Science, and Sustainability. 1st ed., London: CRC Press; 2023, p. 31–6. https://doi.org/10.4324/9781003388982-7.
26. Chen L, Yuan C, Gao B, Chen S, Zhang X. Microwave-assisted synthesis of organic–inorganic poly(3,4-ethylenedioxythiophene)/RuO_2·xH_2O nanocomposite for supercapacitor. J Solid State Electrochem 2009; 13:1925–33. https://doi.org/10.1007/s10008-008-0777-y.
27. Mylarappa M, Chandruvasan S, Harisha KS, Sharath SC. Synthesis, characterization and electrochemical detection of tartaric acid and grape juice using rGO doped La_2O_3 nanoparticles. Materials Science and Engineering: B. 2024; 299:116977. https://doi.org/10.1016/j.mseb.2023.116977.
28. Wang Y, Herron N. Nanometer-sized semiconductor clusters: materials synthesis, quantum size effects, and

photophysical properties. J Phys Chem. 1991; 95:525–32. https://doi.org/10.1021/j100155a009.

29. Mylarappa M, Chandruvasan S, Shravana kumara K N, Sandhya R. Antioxidant, Electrochemical, Photocatalysis and Sensor Studies of rGO Incorporated MgO Nanocomposite. In Review; 2023. https://doi.org/10.21203/rs.3.rs-3378654/v1.
30. Shubha MB, Manjunatha C, Sudeep M, Chandruvasan S, Sumira Malik and Praveen Sekhar. Development of $NiCoO_2$ nanoparticles based electrochemical sensor with extremely low detection for hazardous 4-nitrophenol. J Electrochem Soc. 2023; 170:067509. https://doi.org/10.1149/1945-7111/acdf89.